



## Solid-State NMR Study of Ion-Exchange Processes in $V_2O_5$ Xerogel, Polyaniline/ $V_2O_5$ , and Sulfonated Polyaniline/ $V_2O_5$ Nanocomposites

G. P. Holland,<sup>a</sup> J. L. Yarger,<sup>a</sup> D. A. Buttry,<sup>a,\*</sup> F. Huguenin,<sup>b</sup> and R. M. Torresi<sup>c</sup>

<sup>a</sup>Department of Chemistry, University of Wyoming, Laramie, Wyoming, 82071-3838, USA

<sup>b</sup>Instituto de Química de São Carlos, Universidade de São Paulo, 13560-970 São Carlos (SP), Brazil

<sup>c</sup>Instituto de Química, Universidade de São Paulo, 05513-970 São Paulo (SP), Brazil

The local lithium environment in electrochemically lithiated  $V_2O_5$  xerogel, polyaniline/ $V_2O_5$ , and sulfonated polyaniline/ $V_2O_5$  nanocomposites is probed with solid-state  $^7\text{Li}$  static and magic angle spinning (MAS) nuclear magnetic resonance (NMR). The line width from the static NMR spectra reveals differences between the lithium environments in the three materials. The MAS NMR spectrum of the  $V_2O_5$  parent material in its unreduced (as-prepared) state shows the presence of an intrinsic ion-exchange site that can be populated with  $\text{Li}^+$  by simple exposure to  $\text{LiClO}_4$  in propylene carbonate (PC). Following electrochemical lithiation, both ion-exchange and intercalated lithium sites are observed. After lithiation,  $\text{Li}^+$  ions at the ion-exchange site can be displaced by exposure to  $\text{NaClO}_4$  in PC via a simple ion-exchange process. Both the ion-exchange and intercalated sites are observed for a sulfonated polyaniline/ $V_2O_5$  nanocomposite while the polyaniline/ $V_2O_5$  nanocomposite response is dominated by the intercalated lithium site. The results show that charge compensation of the intrinsic negatively charged ion-exchange sites in the  $V_2O_5$  xerogel by conducting polymers used to form the nanocomposites is important in determining the number and type of  $\text{Li}^+$  sites available.

© 2003 The Electrochemical Society. [DOI: 10.1149/1.1624841] All rights reserved.

Manuscript submitted December 20, 2002; revised manuscript received June 17, 2003. Available electronically November 5, 2003.

The recent literature contains numerous studies on the application of transition metal oxides as  $\text{Li}^+$  insertion hosts in rechargeable lithium batteries.  $V_2O_5$  xerogel is a particularly promising material with efficient and reversible insertion of lithium ions at high potentials vs.  $\text{Li}/\text{Li}^+$ , resulting in high specific capacity and energy density.<sup>1-5</sup> However, lower capacities are typically obtained at high current densities due to slow  $\text{Li}^+$  diffusion within the xerogel. Thus, there is a considerable effort to enhance the overall  $\text{Li}^+$  insertion rate in this and related materials. A substantial improvement in the overall  $\text{Li}^+$  insertion rate was obtained for a  $V_2O_5$  aerogel synthesized on sintered nickel fibers.<sup>6</sup> In that case, the rate enhancements were attributed to decreased lithium diffusion distances due to the highly textured nature of the material. In another approach, more rapid  $\text{Li}^+$  insertion was obtained by employing a supercritical drying process to produce aerogel materials with high surface areas and short diffusion path lengths.<sup>7-9</sup> In addition, Spahr *et al.* synthesized  $V_2O_5$  nanotubes to increase the surface area.<sup>10</sup> These structural alterations decrease the diffusion limitations and increase charge storage resulting in higher power density.

Another approach for improving xerogel performance is to prepare nanocomposites with a conducting polymer incorporated within the xerogel matrix. Previous studies have shown that nanocomposites formed from  $V_2O_5$  sol-gel and either polyaniline (PANI)<sup>11-13</sup> or poly(aniline *N*-propane sulfonic acid) (PSPAN)<sup>14</sup> have higher charge capacity than the xerogel parent material. A higher  $\text{Li}^+$  insertion rate is achieved in these nanocomposites resulting in increased charge storage capacities compared to the untreated xerogel.<sup>15</sup> Specifically, the intercalation rate increases in PANI/ $V_2O_5$  due to an enhancement of  $\text{Li}^+$  mobility.<sup>13,16</sup> Moreover, decreased diffusion path lengths also can improve the overall rate of  $\text{Li}^+$  insertion into the material. It was shown that the diffusion path length is shorter in the PSPAN/ $V_2O_5$  nanocomposite than in  $V_2O_5$  xerogel, increasing the mass-transport rate and the specific capacity of the cathode.<sup>14</sup>

A key issue for understanding the behavior of both  $V_2O_5$  xerogels and nanocomposites incorporating them relates to how the details of the xerogel structure influences the resulting properties of the

materials, especially with regard to  $\text{Li}^+$  diffusion and binding sites. A recent X-ray diffraction (XRD) study using atomic pair distribution function analysis<sup>17</sup> showed that the structure of  $V_2O_5$  xerogel ribbons is based on bilayers of single  $V_2O_5$  layers with square pyramidal  $\text{VO}_5$  units in which the vanadium centers in a given layer achieve pseudo-octahedral coordination by interaction with basal oxygens in the opposing layer. The questions that remain include the nature of the termination of the bilayer slabs and the number and types of  $\text{Li}^+$  sites that are present at these termini and between the bilayer slabs. Understanding the nature of such interfacial  $\text{Li}^+$  sites is even more important when nanostructured cathode materials are used,<sup>18-20</sup> since they have a higher proportion of interfacial sites than traditional materials.

A challenge in working with nanocomposites and nanostructured materials derives from difficulties in obtaining adequate structural characterization, especially given that they often lack long-range order. XRD can yield valuable information regarding structural changes that occur in the host material during  $\text{Li}^+$  insertion.<sup>21</sup> Unfortunately, the poor crystallinity of organic-inorganic hybrid nanocomposites reduces the applicability of this technique.<sup>15,22</sup> In contrast, solid-state nuclear magnetic resonance (NMR) can probe the local environment of a given species in completely amorphous materials. Therefore, it is an especially attractive tool for the highly disordered materials that often result from nanocomposite preparations. Also, since NMR is specific to a particular nucleus, it can be used to probe the local environment experienced by a specific isotope of that nucleus within a given material.<sup>23</sup> In the present study,  $^7\text{Li}$  NMR spectroscopy is employed to probe the local lithium environment in  $V_2O_5$  and several nanocomposite materials comprising  $V_2O_5$  and various polyaniline derivatives. Specifically, both static and magic angle spinning (MAS)  $^7\text{Li}$  NMR spectra are presented for  $V_2O_5$ , PANI/ $V_2O_5$ , and PSPAN/ $V_2O_5$  containing various amounts of ion-exchanged and electrochemically intercalated  $\text{Li}^+$ . Electrochemical data, as well as characterization using a variety of other techniques (Fourier transform infrared spectroscopy, electrochemical quartz crystal microbalance, electroacoustic impedance, *in situ* resistance, X-ray diffraction, thermal gravimetric analysis, and differential scanning calorimetry) have been presented previously for

\* Electrochemical Society Active Member.

<sup>z</sup> E-mail: Buttry@uwyo.edu

$V_2O_5$  and the PANI/ $V_2O_5$  composite<sup>13</sup> and for the PSPAN/ $V_2O_5$  composite,<sup>15</sup> so those data are not reproduced here.

### Experimental

$V_2O_5 \cdot nH_2O$  was synthesized following a variation of a previously described sol-gel method<sup>4</sup> in which vanadyl tris(isopropoxide),  $VC_9H_{21}O_4$  (Gelest), is added to excess water resulting in spontaneous formation of  $V_2O_5$  sol-gel. Nanocomposites of  $[PANI]_{0.3}V_2O_5$  were produced by adding 0.2 mL of  $VC_9H_{21}O_4$  to a solution of 120 mL of water and  $11.5 \times 10^{-3}$  mL of aniline. Nanocomposites of  $[PSPAN]_{0.3}V_2O_5$  were produced by addition of 0.2 mL of  $VC_9H_{21}O_4$  to 120 mL of an aqueous solution containing 30 mg of *N*-propane sulfonic acid aniline.<sup>24</sup> These systems were heated in a rotary evaporator at 40°C under vacuum for 4 h to obtain viscous gels that could be cast on stainless steel electrodes and dried. The notation used ( $[conducting\ polymer]_x V_2O_5$ ) to describe the composition of the nanocomposites gives the number of aniline rings ( $x$ ) per  $V_2O_5$  formula unit, as previously discussed.<sup>15</sup>

Lithium ions were exchanged with cationic species within the as-formed  $V_2O_5$  xerogel via an ion exchange process by immersion of the xerogel sample into a 1.0 M solution of  $LiClO_4$  in propylene carbonate (PC) in an Ar-filled dry box (Vacuum Atmospheres). Immersion times were typically several hours. Following the ion-exchange process the samples were immersed in pure PC for two days to remove extraneous supporting electrolyte, followed by copious rinsing and drying under dynamic vacuum at a temperature of 100°C.

Electrochemical lithium ion insertion was accomplished by performing potentiostatic step experiments with a EG&G PAR (Princeton Applied Research) 273 potentiostat. The electrochemical experiments were performed in an argon-filled glove box (Vacuum Atmospheres). The working electrode was a piece of stainless steel mesh with a geometrical surface area of 40 cm<sup>2</sup> dip-coated with the formed gels. The coated electrodes were annealed at 100°C in a vacuum oven. Both the reference and auxiliary electrodes were lithium metal. The electrolyte used was 1.0 M  $LiClO_4$  in propylene carbonate (PC). Lithium ions were electrochemically inserted by applying potential steps between 1.8 and 3.5 V (vs.  $Li/Li^+$ ) depending on the desired amount of intercalation. The lithiated samples were rinsed with clean PC to remove the supporting electrolyte following the electrochemical process. The rinsed samples were placed on a high vacuum line where the PC was removed at 100°C under high vacuum.

Sodium ion was exchanged into electrochemically lithiated  $V_2O_5$  xerogel using the same procedure described above for  $Li^+$  except with 1.0 M  $NaClO_4$  rather than  $LiClO_4$ . Samples were exposed to the  $NaClO_4$  solution for various times to examine the time dependence of the exchange process. After rinsing with pure PC and drying, each sample was examined using  $^7Li$  MAS NMR.

NMR measurements were carried out with a Bruker MSL-400 spectrometer employing a 4 mm Bruker VT-MAS probe operating at a  $^7Li$  frequency of 155.5 MHz. A one-pulse sequence was used, with a pulse length of 3  $\mu$ s, a recycle delay of 500 ms (due to the short  $T_1$  relaxation times), and a minimum of 100,000 scans. All nanocomposite samples were run overnight. The samples were removed from the stainless steel mesh and packed in zirconia rotors with Kel-F caps in a glove box to avoid contamination of the air-sensitive lithiated samples. MAS experiments were performed at a rotor-spinning rate ( $\omega_R$ ) of 10 kHz  $\pm$  5 Hz. In spite of the lengthy data acquisition times for the spectra, a less than ideal signal-to-noise ratio (S/N) observed in the NMR spectra for several of the nanocomposite samples was observed due to the small amount of sample available (0.5-2 mg) following electrochemical  $Li^+$  insertion, solvent rinsing, and high vacuum drying. The peaks in the NMR spectra were fit to one or two Lorentzians for static and MAS spectra, respectively, to obtain accurate values for the full width at half maximum (fwhm) and chemical shift.

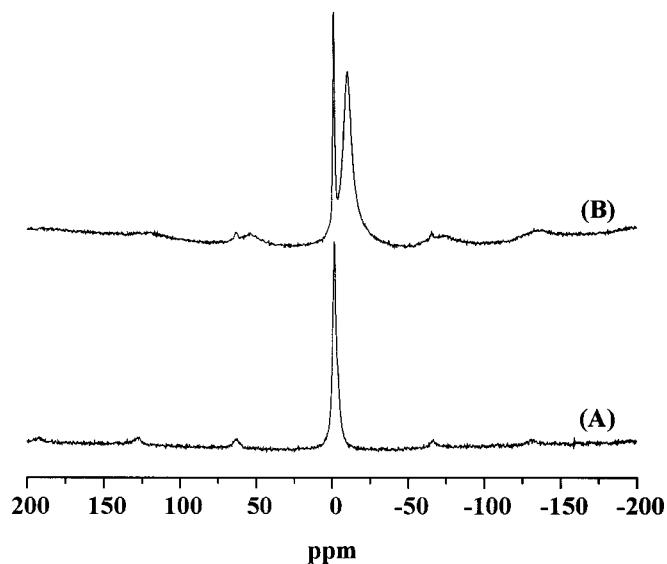


**Figure 1.** Room temperature MAS  $^7Li$  NMR spectra of (A) ion-exchanged  $V_2O_5$  xerogel and (B) electrochemically lithiated  $Li_{0.2}V_2O_5$  xerogel.

### Results and Discussion

*$V_2O_5$  xerogel.*—Figure 1A shows the  $^7Li$  MAS NMR spectrum for an as-formed  $V_2O_5$  xerogel sample following exposure to 1.0 M  $LiClO_4$ , rinsing with PC, and drying. Under rapid MAS conditions, first-order quadrupole effects, nuclear magnetic dipolar effects, and anisotropic shift interactions are averaged to zero.<sup>25,26</sup> The spectrum shows a narrow resonance positioned near 0 ppm along with weak spinning sidebands corresponding to the satellite transitions at  $\pm\omega_R = 10$  kHz. This peak is in a position typical for ionic lithium. Livage *et al.* have shown that a small percentage of  $V^{4+}$  sites produced during sol-gel synthesis of  $V_2O_5$  are charge compensated by protons.<sup>4</sup> Others have shown that these protons can be ion-exchanged for metal cations by simple immersion into a PC solution containing the cation of interest.<sup>27-29</sup> Thus, we assign this resonance to  $Li^+$  in an ion-exchange site at the surface of the  $V_2O_5$  ribbons.

Figure 1B shows the  $^7Li$  MAS spectrum for an electrochemically lithiated  $Li_{0.2}V_2O_5$  xerogel sample. This spectrum shows both a sharp peak near 0 ppm and a broader, upfield peak at *ca.* -10 ppm. These resonances are assigned to ion-exchanged  $Li^+$  and intercalated  $Li^+$ , respectively, consistent with previous assignments.<sup>23</sup>  $^7Li$  MAS spin-lattice ( $T_1$ ) relaxation measurements give a relaxation time of  $115 \pm 10$  ms for the sharper peak. This lifetime is substantially shorter than that for common lithium salts and lithium in solid electrolyte interphase (SEI) films, which are typically  $\geq 1$  s.<sup>30</sup> As previously discussed, this short lifetime shows that this peak does not derive from an impurity phase. The broader peak shifts farther upfield and broadens with increasing lithiation. It has a  $T_1$  relaxation time of  $20 \pm 2$  ms, indicating a substantial spin-lattice relaxation rate compared to that for ionic lithium in simple salts. Paramagnetic shifts also have been reported for lithium in lithiated crystalline vanadium oxides.<sup>31,32</sup> For the xerogel material, this behavior has been attributed to a dipolar pseudocontact interaction between the  $^7Li$  nuclei and unpaired electrons present at  $V^{4+}$  sites. For the static spectra the dependence of the  $T_1$  relaxation time was used with  $Li^+$  diffusion measurements<sup>33</sup> and previously reported polaron hopping rates<sup>34</sup> to unequivocally demonstrate coupling between the Li nuclei and polarons in the  $V_2O_5$  lattice.<sup>23</sup> The small response that is observed as a shoulder on the upfield side of the ion-exchange peak in Fig. 1A may be due to a small population of intercalated  $Li^+$ .

The results of time-dependent ion-exchange experiments in which  $Li^+$  was replaced by  $Na^+$  are summarized in Fig. 2. For these

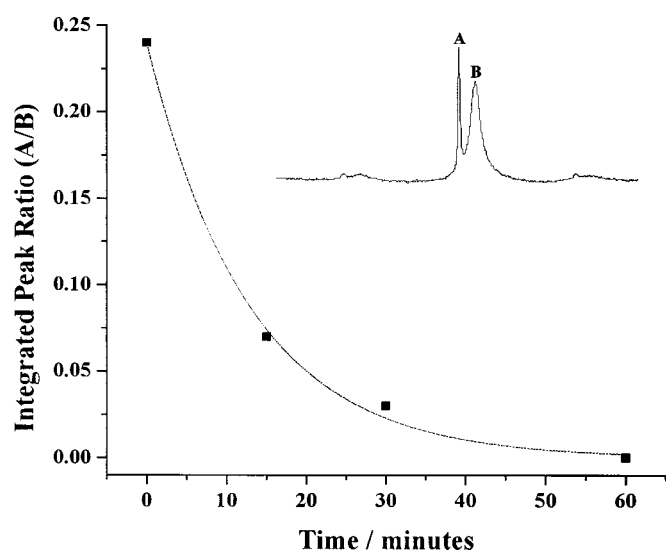


**Figure 2.** Time dependence of ion-exchange in  $\text{Li}_{0.2}\text{V}_2\text{O}_5$  xerogel exposed to 1 M  $\text{NaClO}_4$  in PC plotted as the integrated peak ratio (A/B) as a function of exposure time in minutes.

experiments, electrochemically lithiated  $\text{V}_2\text{O}_5$  samples were exposed to 1.0 M  $\text{NaClO}_4$  in PC for various times, rinsed with pure PC, and dried. Then, the  $^7\text{Li}$  MAS NMR peak intensities for the ion-exchanged and intercalated  $\text{Li}^+$  components were quantitatively evaluated for each sample. These data are plotted in the figure as the ratio of the intensity for the ion-exchanged  $\text{Li}^+$  component to that for the intercalated  $\text{Li}^+$  component as a function of time, where the ratio is used to eliminate the need to compare absolute intensities for each of the samples. These results show that the ion-exchanged  $\text{Li}^+$  component is much more rapidly replaced by  $\text{Na}^+$  than the intercalated  $\text{Li}^+$ , with a half-life of 12.8 min. The faster ion-exchange rate shown in Fig. 2 is entirely consistent with the much better accessibility expected for the ion-exchange  $\text{Li}^+$  sites compared to the intercalation sites.

**Conducting polymer/ $\text{V}_2\text{O}_5$  nanocomposites.**— $^7\text{Li}$  static NMR spectra for  $\text{Li}_{1.3}\text{V}_2\text{O}_5$ ,  $\text{Li}_{1.3}[\text{PSPAN}]_{0.3}\text{V}_2\text{O}_5$ , and  $\text{Li}_{1.3}[\text{PANI}]_{0.3}\text{V}_2\text{O}_5$  are shown in Fig. 3. A single broad resonance is observed for all three samples. Satellite transitions ( $\pm 3/2 \leftrightarrow \pm 1/2$ ) that are often observed in  $^7\text{Li}$  ( $I = 3/2$ ) solid-state NMR spectra due to the quadrupole interaction are not evident in any of the spectra. This is consistent with previous observations for lithiated  $\text{V}_2\text{O}_5$  xerogel.<sup>23</sup> The fwhm values for the broad resonances are 19, 31, and 40 kHz for  $\text{Li}_{1.3}\text{V}_2\text{O}_5$ ,  $\text{Li}_{1.3}[\text{PANI}]_{0.3}\text{V}_2\text{O}_5$ , and  $\text{Li}_{1.3}[\text{PSPAN}]_{0.3}\text{V}_2\text{O}_5$ , respectively. These data show a larger line width for the nanocomposite materials compared to the xerogel parent material at an identical degree of lithiation. However, it should be noted that the synthetic procedures described in the Experimental section lead to reduction of  $\text{V}^{5+}$  to  $\text{V}^{4+}$  during the oxidative polymerization of the aniline monomers.<sup>35,36</sup> This is borne out in the open-circuit potentials (OCP) for the various samples prior to electrochemical lithiation, which are 3.9, 3.8, and 3.7 V for the xerogel, xerogel/PANI, and xerogel/PSPAN materials, respectively. The lower OCP values for the conducting polymer nanocomposites show that they contain substantial numbers of  $\text{V}^{4+}$  centers before any lithiation is done, meaning that at a given degree of lithiation the nanocomposites contain more  $\text{V}^{4+}$  centers than the xerogel parent material. Thus, electron-nuclear coupling between the  $^7\text{Li}$  nuclei and paramagnetic electrons at these reduced vanadium sites is one possible origin of the observed line broadening in the nanocomposites. Another possible source of increased line widths for the nanocomposites would be dipolar coupling between the  $^7\text{Li}$  nuclei and para-

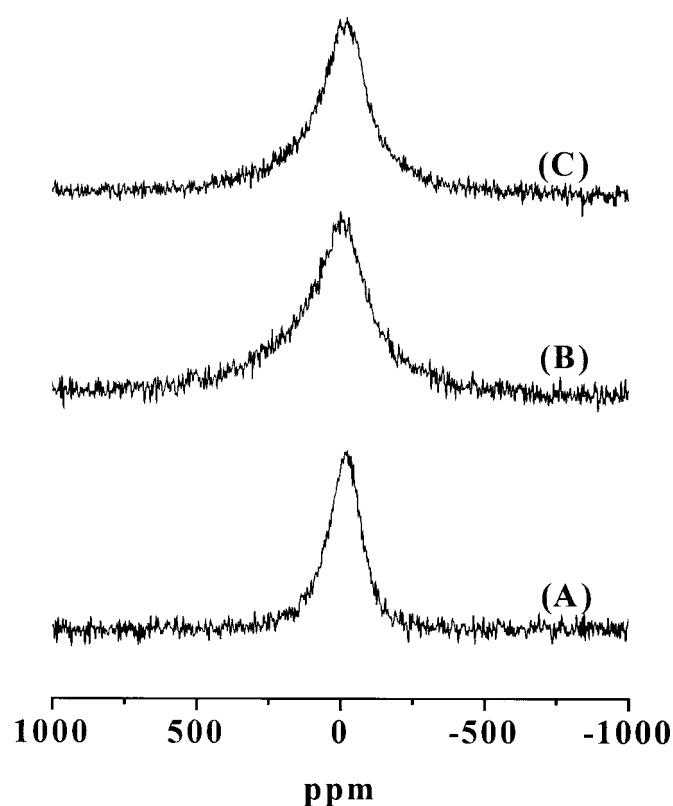
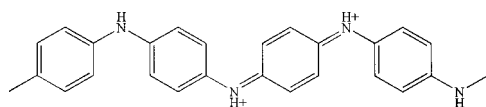


**Figure 3.** Room temperature static  $^7\text{Li}$  NMR spectra of electrochemically lithiated (A)  $\text{Li}_{1.3}\text{V}_2\text{O}_5$ , (B)  $\text{Li}_{1.3}[\text{PANI}]_{0.3}\text{V}_2\text{O}_5$ , and (C)  $\text{Li}_{1.3}[\text{PSPAN}]_{0.3}\text{V}_2\text{O}_5$ .

magnetic sites on the doped conducting polymer chains. However, previous solid-state NMR studies of doped polyaniline showed that electron spins on the conducting polymer chains did not contribute substantially to the broadening of  $^{13}\text{C}$  and  $^{14}\text{N}$  signals.<sup>37</sup> This suggests that this mechanism probably should not be operative for the  $^7\text{Li}$  spins in the present case. One other possible source of broadening for the nanocomposites is  $^7\text{Li}$ - $^1\text{H}$  dipolar coupling, where the protons are those on the conducting polymer chains. Previous XRD data on a  $[\text{PANI}]_{0.3}\text{V}_2\text{O}_5$  nanocomposite prepared identically to those studied here indicate that the conducting polymer is not present in the interlayer region.<sup>13</sup> In contrast, XRD data for a  $[\text{PSPAN}]_{0.15}\text{V}_2\text{O}_5$  nanocomposite demonstrated intercalation of the polymer chains within the interlayer region.<sup>15</sup> The origin of this difference is not clear. However, the fact that these structurally different materials give linewidths that track the  $\text{V}^{4+}$  population (as the OCP) suggests strongly that linewidths are dominated by electron-nuclear coupling as in  $\text{V}_2\text{O}_5$ . Thus, we assign the increased broadening in the nanocomposite samples to stronger interactions between the  $^7\text{Li}$  nuclei and the increased number of  $\text{V}^{4+}$  centers present in these samples compared to the parent xerogel material.

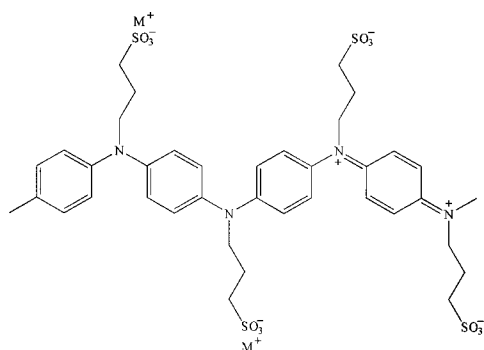
$^7\text{Li}$  MAS NMR spectra of the  $\text{Li}_x[\text{PANI}]_{0.3}\text{V}_2\text{O}_5$  composite are presented in Fig. 4 for (A)  $x = 0.3$  and (B)  $x = 0.7$ . The spectrum at low  $\text{Li}^+$  loading shows only a very small amount of the ion-exchange component (minor, narrow peak at 0 ppm) and a substantial amount of the intercalated  $\text{Li}^+$  component (broad, upfield peak at ca.  $-20$  ppm). For the  $x = 0.7$  case, the ion-exchange component is almost completely absent and the  $^7\text{Li}$  spectrum is dominated by the broad peak. This is understandable based on the PANI structure shown in Scheme I. As is widely known, the doped, conductive



Scheme I.

state of PANI is cationic, causing it to function as an anion exchange material.<sup>38</sup> Hence, we interpret the lack of a substantial amount of ion-exchanged  $\text{Li}^+$  in these samples as indicating that the anionic, ion-exchange sites on the  $\text{V}_2\text{O}_5$  xerogel ribbons are charge-compensated by cationic charges from doped PANI chains produced during synthesis. However, during doping, the insertion of additional negative charge as the matrix is reduced creates a requirement for additional cationic charge that is filled by  $\text{Li}^+$  insertion into the material, giving rise to the broadened peak that is shifted upfield.

$^7\text{Li}$  MAS NMR spectra of  $\text{Li}_x[\text{PSPAN}]_{0.3}\text{V}_2\text{O}_5$  containing two different amounts of intercalated  $\text{Li}^+$  are shown in Fig. 5. These spectra clearly show the presence of a considerable amount of  $\text{Li}^+$  in the ion-exchange site (strong peak at 0 ppm), as well as intercalated  $\text{Li}^+$  (broader peak at *ca.* -20 ppm). Again, this result can be understood based on the structure for PSPAN that is shown in Scheme II.



Scheme II.

PSPAN is a self-doped conducting polymer, meaning that it possesses pendent anionic groups that can provide charge compensation during doping of the polyaniline-like groups in the main chains. Previous work with a related, partially sulfonated polyaniline derivative has demonstrated that a major fraction of the charge compensation during doping is achieved by cation transport.<sup>39</sup> Thus, one expects that a PSPAN/ $\text{V}_2\text{O}_5$  nanocomposite should contain  $\text{Li}^+$  to provide charge compensation both for the anionic sites on the  $\text{V}_2\text{O}_5$  ribbons and for the pendent sulfonate groups on the PSPAN chains. The strong signal observed at 0 ppm for the  $\text{Li}_x[\text{PSPAN}]_{0.3}\text{V}_2\text{O}_5$  samples provides good evidence for this. Interestingly, the relative increase in the spectral intensity for  $\text{Li}^+$  in the ion-exchange site for the  $x = 0.7$  case suggests that at least some of the charge compensation during doping is achieved via  $\text{Li}^+$  association with the pendent sulfonate groups, as expected for a self-doped material like PSPAN.

### Conclusions

This study has demonstrated that  $\text{Li}^+$  is present in ion-exchange sites in both  $\text{V}_2\text{O}_5$  xerogels and in nanocomposites formed from  $\text{V}_2\text{O}_5$  and PSPAN. For the un lithiated parent xerogel, this ion-exchanged  $\text{Li}^+$  is coupled via dipolar interactions with paramagnets that are most likely  $\text{V}^{4+}$  centers produced during the sol-gel drying process.<sup>4</sup> For the PSPAN/ $\text{V}_2\text{O}_5$  material, the ion-exchanged  $\text{Li}^+$  may be associated either with anionic sites on the  $\text{V}_2\text{O}_5$  ribbons or

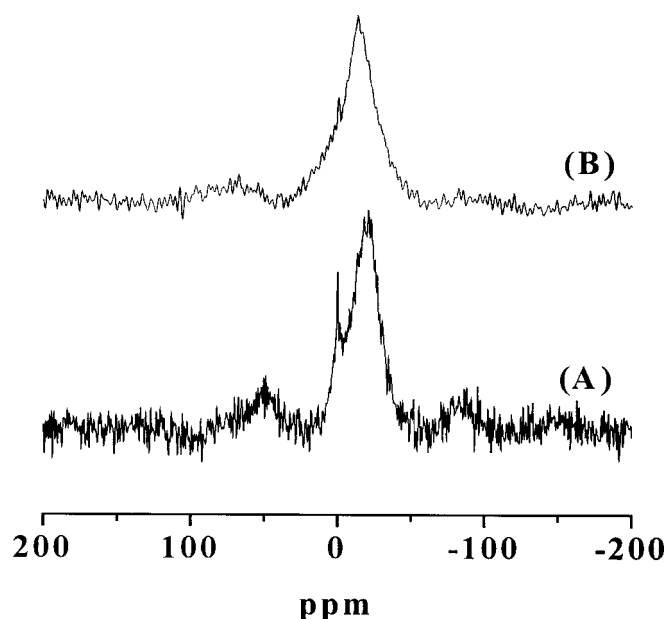


Figure 4. Room temperature MAS  $^7\text{Li}$  NMR spectra of electrochemically lithiated  $\text{Li}_x[\text{PANI}]_{0.3}\text{V}_2\text{O}_5$ , (A)  $x = 0.3$  and (B) 0.7. A spinning speed of 10 kHz was used for both samples.

with pendent sulfonate groups on the polymer. For nanocomposites comprised of both  $\text{V}_2\text{O}_5$  and PANI, the ion-exchanged  $\text{Li}^+$  component is almost entirely absent. The results for the nanocomposites are consistent with the charge compensation expected based on the structures of the two conducting polymers, and on previous results for similar materials.<sup>15,39</sup> These results show that the notions of self-doping for conducting polymers can be equally well applied to nanocomposites. They also show the power of solid-state NMR when used for descriptive studies in such materials.

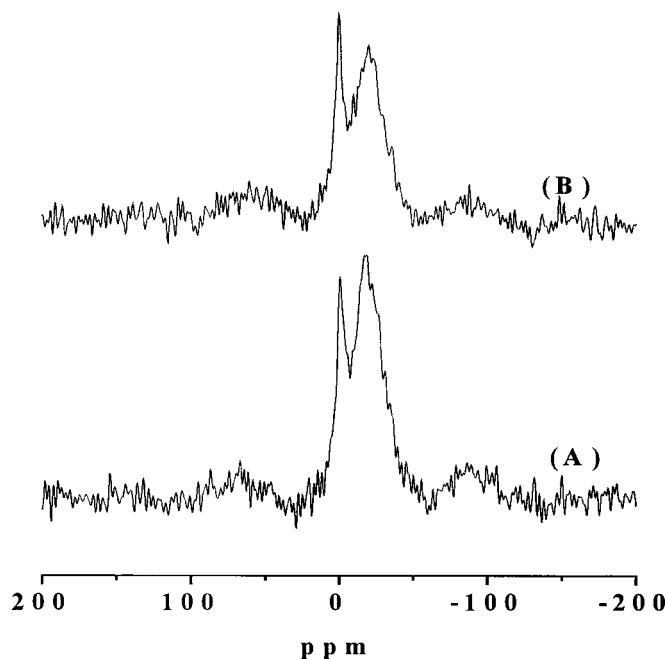


Figure 5. Room temperature MAS  $^7\text{Li}$  NMR spectra of electrochemically lithiated  $\text{Li}_x[\text{PSPAN}]_{0.3}\text{V}_2\text{O}_5$ , (A)  $x = 0.3$  and (B) 0.7. A spinning speed of 10 kHz was used for both samples.

### Acknowledgments

We are grateful to FAPESP and CNPq (process no. 910043/97-3) (Brazilian Agencies) for support of the work at USP and the National Science Foundation (INT-9724792), the Department of Energy (DE-FG02-00ER45836 and DE-FG03-01ER15250) and National Science Foundation (CAREER Award CHE-0094202 and CHE-0092041) for support of the work at U.W. F. H. acknowledges FAPESP scholarship no. 98/15848-3.

University of Wyoming assisted in meeting the publication costs of this article.

### References

- J.-P. Pereira-Ramos, *J. Power Sources*, **54**, 120 (1995).
- H.-K. Park, W. H. Smyrl, and M. D. Ward, *J. Electrochem. Soc.*, **142**, 1068 (1995).
- A. L. Tipton, S. Passerini, B. B. Owens, and W. H. Smyrl, *J. Electrochem. Soc.*, **143**, 3473 (1996).
- J. Livage, *Chem. Mater.*, **3**, 578 (1991).
- H. Varela, F. Huguenin, M. Malta, and R. M. Torresi, *Quim. Nova*, **25**, 287 (2002).
- M. J. Parent, S. Passerini, B. B. Owens, and W. H. Smyrl, *J. Electrochem. Soc.*, **146**, 1346 (1999).
- D. B. Lê, S. Passerini, A. L. Tipton, B. B. Owens, and W. H. Smyrl, *J. Electrochem. Soc.*, **142**, L102 (1995).
- F. Coustier, S. Passerini, and W. H. Smyrl, *J. Electrochem. Soc.*, **145**, L73 (1998).
- W. Dong, D. R. Rolison, and B. Dunn, *Electrochem. Solid-State Lett.*, **3**, 457 (2000).
- M. E. Spahr, P. Stoschitzki-Bitterli, R. Nesper, O. Haas, and P. Novák, *J. Electrochem. Soc.*, **146**, 2780 (1999).
- F. Leroux, B. E. Koene, and L. F. Nazar, *J. Electrochem. Soc.*, **143**, L181 (1996).
- M. Lira-Cantú and P. Gómez-Romero, *J. Electrochem. Soc.*, **146**, 2029 (1999).
- F. Huguenin, R. M. Torresi, and D. A. Buttry, *J. Electrochem. Soc.*, **149**, A546 (2002).
- F. Huguenin, R. M. Torresi, D. A. Buttry, J. E. P. d. Silva, and S. I. C. d. Torresi, *Electrochim. Acta*, **46**, 3555 (2001).
- F. Huguenin, M. T. P. Gambardella, R. M. Torresi, S. I. C. d. Torresi, and D. A. Buttry, *J. Electrochem. Soc.*, **147**, 2437 (2000).
- F. Leurox, G. Goward, W. P. Power, and L. F. Nazar, *J. Electrochem. Soc.*, **144**, 3886 (1997).
- V. Petkov, P. N. Trikalitis, E. S. Bozin, S. J. L. Billinge, T. Vogt, and M. G. Kanatzidis, *J. Am. Chem. Soc.*, **124**, 10157 (2002).
- G. G. Amatucci, F. Badway, A. Singhal, B. Beaudoin, G. Skandan, T. Bowmer, I. Plitz, N. Pereira, T. Chapman, and R. Jaworski, *J. Electrochem. Soc.*, **148**, A940 (2001).
- D. Im and A. Manthiram, *J. Electrochem. Soc.*, **149**, A1001 (2002).
- P. Lucas and C. A. Angell, *J. Electrochem. Soc.*, **147**, 4459 (2000).
- E. A. Meulenkamp, W. v. Klinken, and A. R. Schlattmann, *Solid State Ionics*, **126**, 235 (1999).
- P. Gómez-Romero, *Adv. Mater. (Weinheim, Ger.)*, **13**, 163 (2001).
- G. P. Holland, D. A. Buttry, and J. L. Yarger, *Chem. Mater.*, **14**, 3875 (2002).
- F. Huguenin, M. J. Giz, E. A. Ticianelli, and R. M. Torresi, *J. Power Sources*, **103**, 113 (2001).
- M. D. Meadows, K. A. Smith, R. A. Kinsey, T. M. Rothgeb, R. P. Skarjune, and E. Oldfield, *Proc. Natl. Acad. Sci. U.S.A.*, **79**, 1351 (1982).
- I. J. Lowe, *Phys. Rev. Lett.*, **2**, 285 (1959).
- R. Baddour, J. P. Pereira-Ramos, R. Messina, and J. Perichon, *J. Electroanal. Chem.*, **81**, 314 (1991).
- L. Znaidi, N. Baffier, and D. Lemordant, *Solid State Ionics*, **28-30**, 1750 (1988).
- R. Baddour, J. P. Pereira-Ramos, R. Messina, and J. Perichon, *J. Electroanal. Chem.*, **277**, 359 (1990).
- Y. Wang, X. Guo, S. Greenbaum, J. Liu, and K. Amine, *Electrochem. Solid-State Lett.*, **4**, A68 (2001).
- J. Hirschinger, T. Mongrelet, C. Marichal, P. Granger, J. Savariault, E. Déramond, and J. Galy, *J. Phys. Chem.*, **97**, 10301 (1993).
- P. E. Stallworth, F. S. Johnson, S. G. Greenbaum, S. Passerini, J. Flowers, W. Smyrl, and J. J. Fontanella, *Solid State Ionics*, **146**, 43 (2002).
- G. P. Holland, F. Huguenin, R. M. Torresi, and D. A. Buttry, *J. Electrochem. Soc.*, **150**, A721 (2003).
- M. Murawski, C. Sanchez, J. Livage, and J. P. Audiere, *J. Non-Cryst. Solids*, **124**, 71 (1990).
- M. G. Kanatzidis, C. G. Wu, H. O. Marcy, and C. R. Kannewurf, *J. Am. Chem. Soc.*, **111**, 4139 (1989).
- C. G. Wu, D. C. DeGroot, H. O. Marcy, J. L. Schindler, C. R. Kannewurf, Y. J. Liu, W. Hirpo, and M. G. Kanatzidis, *Chem. Mater.*, **8**, 1992 (1996).
- S. Kababya, M. Appel, Y. Haba, G. I. Titelman, and A. Schmidt, *Macromolecules*, **32**, 5357 (1999).
- D. Orata and D. A. Buttry, *J. Am. Chem. Soc.*, **109**, 3574 (1987).
- H. Varela, R. M. Torresi, and D. A. Buttry, *J. Electrochem. Soc.*, **147**, 4217 (2000).